






# Optimization of Processing Parameters and Mechanical Properties of SLM Titanium Alloy

Jammula Praneeth<sup>(✉)</sup> , Sriram Venatesh , and L. Sivarama Ramarishna 

Osmania University, Hyderabad 500007, Telangana, India  
jpraneeth1202@gmail.com

**Abstract.** A form of additive manufacturing named selective laser melting (SLM) involves a laser to melt and fuse metallic powders together layer by layer to produce solid parts. In SLM, a number of variables, including laser power, scan speed, layer thickness, and hatch spacing, can influence the final product's quality and precision. The best values for these factors to produce the desired qualities in the finished product are commonly found through experimental investigations. In this investigation, we produced titanium alloy pieces from the Ti6Al4V ELI material using SLM technique. The effect of three factors, namely laser power, scan speed, and hatch distance, on the density, micro-hardness, and surface roughness of the produced components was systematically studied and optimised using the Taguchi technique, a statistical method for designing and evaluating tests. The signal-to-noise (S/N) ratios, which are a measure of the magnitude of the output signal relative to the level of noise, and ANOVA, a statistical technique used to assess the significance of variations between means, were then employed to examine the results. According to experimental findings, a sample with a density greater than 99.54%, a micro-hardness of 386 HV, and a roughness measurement of 10.86  $\mu\text{m}$  were produced. The process variables that had the greatest impact on the mechanical characteristics of the laser-deposited Ti-6Al-4V alloy were found to be laser power and scanning speed.

**Keywords:** Selective Laser Melting (SLM) · Ti6Al4V ELI · Process Parameters · Energy Density · Properties

## 1 Introduction

Industry is interested in additive manufacturing (AM) techniques because they may produce fully functional complicated geometries from a digital model by attaching material layer by layer [1, 2]. By selectively melting and fusing metallic powder, selective laser melting (SLM) produces high density 3D objects. A 3D geometry's cross sections are successively fused on top of one another in a layer-by-layer fashion. High value sectors like the aerospace industry can process high performance materials with design freedom because to the SLM method [3]. By increasing material use, reducing processing time,

reducing structural weight, and producing complicated structures, additive manufacturing (AM) technology can be utilised to make aircraft parts and components as opposed to conventional manufacturing procedures. One popular AM procedure is selective laser melting (SLM). The presence of deposition layers during the SLM additive manufacturing process may have an impact on the mechanical qualities of the parts and components produced via additive manufacturing, owing to these deposited layers [4]. It nevertheless has drawbacks despite these benefits, the heated powder rapidly cooled because of the features of laser heating. During the cooling process for volume shrinkage, the pores that affected the density and characteristics of the samples were easily produced. As a result, increasing the density of samples created by SLM is difficult. Titanium alloys are used extensively in aircraft. Due to its excellent strength-to-weight ratio, heat resistance, and biocompatibility, it is used in engineering for both biomedical and automotive purposes [5]. Although, because traditional production techniques require a lot of labor-intensive, resource-intensive, and material-intensive processing stages, manufacturing processes have always been the biggest barrier to the further promotion of titanium alloys. With the introduction of additive manufacturing in recent years, this issue has gradually been eliminated (AM). Particularly, the processing of titanium alloy parts has drawn increasing attention to selective laser melting (SLM) technology [6]. A high-power laser is used as the heat source in the recently created additive manufacturing method known as SLM to controlled melting of sequential powder layers in a specified path. Its advantages include rapid net-shape generation and excellent efficiency for metal alloys. Power, scan speed, and powder layer thickness all significantly affect the SLM process' ability to produce objects with the necessary porosity, roughness, and mechanical characteristics [7–9]. In particular, when the powder layer thickness grows, the as-built parts' porosity and top surface roughness increase continually [10]. With varying intervals of laser strength, scan speed, and hatch distance, more complex trends were seen. The porosity of an as-fabricated Ti6Al4V alloy increases and subsequently declines during 1500–4500 mm/s for the scan rate [11, 12], whereas scan rates of 500–1200 mm/s revealed a reduction in porosity [13]. As a result, tests were planned for the objective of systematic design optimization in this work. Based on Gong's recommendations for the ideal parameters for Ti6Al4V samples, A parameter range of about 63 J/mm<sup>3</sup>, a scan speed of 1200 mm/s, and a laser power of 250 W are chosen. [14]. In order to build a theoretical foundation for titanium alloys made by SLM, The relationship between processing parameters, microstructure, and mechanical characteristics is also being investigated.

## 2 Experimental Investigation

A spherical Ti6Al4V ELI powder that had been gas-atomized and had an the typical particle size of 38  $\mu\text{m}$  was the substance employed in this experiment, as shown in Fig. 1. SLM machine SLM Solution 280 HL was used to perform the SLM process, as shown in Fig. 2. This machine uses a single Yb-fiber laser with a spot size of 90 $\mu\text{m}$  in addition to a maximum laser output power of 400W.

Cubic samples of 15  $\times$  15  $\times$  12 mm were created using a 30  $\mu\text{m}$  powder layer thickness, various laser power scan speeds, and hatch space. Table 1 lists the particular process parameters and their levels. With a continuous laser mode and a checkerboard pattern that alternated by 60° between each succeeding layer, the layers were scanned.

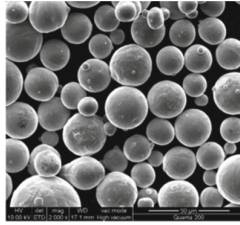


**Fig. 1:** SEM images of the Ti6Al4V powder



**Fig. 2:** SLM 280

**Table 1.** Parameters and their levels for laser powder deposition Ti6Al4V ELI

Parameters	Level 1	Level 2	Level 3
Laser power (W)	250	300	350
Laser scanning speed (V, mm/s)	1000	1200	1400
Hatch space	90	100	110

Argon is employed as a shielding gas, and the platform was maintained at 200 °C. Substrate plate was removed from the machine once the process was finished, and samples were sliced using a multicutting tool.

### 3 Results and Discussion

#### 3.1 Variation of Relative Density

The density of the samples was measured using Archimedes' method. The relative density of each sample was calculated as the sample density divided by the density of water. During the trials, distilled water was utilised to achieve the required buoyancy. The water was 25 °C in temperature. Since it is possible for air bubbles to stick to the surface while the sample is submerged in the water, the densities were measured only after the bubbles had been carefully seen and eliminated. With a precision of 0.1 mg, in both the water and the air, the weight was electronically measured. Five measurements have been made of each sample to reduce measurement error at random and uncertainty. The samples'

**Table 2:** Density Test Values

S.no	Power W	Laser Scan Speed mm/s	Hatch space $\mu\text{m}$	Layer height ( $\mu\text{m}$ )	Laser Energy Density in $\text{J}/\text{mm}^3$	Density of samples ( $\text{g}/\text{cm}^3$ )
1	250	1000	90	30	93	4.304
2	300	1200	100	30	83	4.302
3	350	1400	110	30	76	4.398
4	250	1200	110	30	63	4.410
5	300	1400	90	30	79	4.356
6	350	1000	100	30	117	4.301
7	250	1400	100	30	60	4.406
8	300	1000	110	30	91	4.303
9	350	1200	90	30	108	4.312

densities ( $\rho_s$ ) were estimated using Eq. (1) [12].

$$\rho = w_a \times \rho_w / (W_a - W_w) \quad (1)$$

where  $W_a$  stands for the sample's weight in air,  $W_w$  for the sample's weight in water, and  $w$  for the water's density. By comparing the observed densities to the Ti-6Al-4V ELI alloy's average bulk density  $4.430 \text{ g}/\text{cm}^3$ , the relative densities of the specimen samples produced with several energy densities (ED's) were computed. The densities of the samples have shown a considerable energy density (ED) influence. According to the Archimedes' principle, there was a difference of about 2.47% between the samples with the highest and lowest relative densities. The densities of the samples created under various EDs are summarized in Table 2. The sample sets 4 and 6 had a maximum sample density of  $4.410 \text{ g}/\text{cm}^3$  (relative density: 99.54%) and a minimum density of  $4.301 \text{ g}/\text{cm}^3$  (relative density: 97%), respectively, and were produced using  $63 \text{ J}/\text{mm}^3$  and  $117 \text{ J}/\text{mm}^3$  ED, respectively.

The highest and lowest densities were obtained using scanning speeds of  $1200 \text{ mm}/\text{s}$  and  $1000 \text{ mm}/\text{s}$ , respectively. Sample sets 3 and 7 were done at a scanning speed of  $1400 \text{ mm}/\text{s}$ , with an ED range of  $60 \text{ J}/\text{mm}^3$  to  $76 \text{ J}/\text{mm}^3$ , and both have relative densities exceeding 99%. The powdered Ti-6Al-4V particles were completely dense. Therefore, the development of porosity results from During the samples' melting and solidification, voids formed.

### 3.2 Microhardness

In Table 3, shows the specimens' microhardness values are in relation to various Energy densities. Building height increases cause a drop in microhardness levels. This is mostly due to the fact that the bottom layers' cooling rate and temperature gradient are higher than those of the Centre and top layers', leading to finer cells and higher residual stress,

**Table 3:** Microhardness Test Values

S.no	Power W	Laser Scan Speed mm/s	Hatch space $\mu\text{m}$	Layer height ( $\mu\text{m}$ )	Laser Energy Density in $\text{J}/\text{mm}^3$	Microhardness MH
1	250	1000	90	30	93	380
2	300	1200	100	30	83	383
3	350	1400	110	30	76	385
4	250	1200	110	30	63	386
5	300	1400	90	30	79	382
6	350	1000	100	30	117	379
7	250	1400	100	30	60	384
8	300	1000	110	30	91	378
9	350	1200	90	30	108	377

which in turn increases the microhardness. A 5kg force was applied to a hardness tester during the Vickers hardness tests. Each sample's average hardness was determined by taking five indentations spaced five millimeter apart along the width of a  $15 \times 15 \times 12$  mm block cross section. The maximum hardness of 386 HV for sample specimen 5 was attained using the following parameters, power of 250W, scan speed of 1200 mm/s, hatch spacing of 110  $\mu\text{m}$ , layer space of 30  $\mu\text{m}$ , as well as a the density of laser energy 63  $\text{J}/\text{mm}^3$ . The scan speed was 1200 mm/s, the hatch distance was 90  $\mu\text{m}$ , and the layer height was 30  $\mu\text{m}$ . The minimum Microhardness 377 HV observed for test sample 9 has an energy density of 108  $\text{J}/\text{mm}^3$ .

### 3.3 Surface Roughness

The obtained measurements from the measuring of front face surface roughness are shown in Table 4. (Ra). According to the information's average surface roughness (Ra), the test specimen 6 had an energy density of 117  $\text{J}/\text{mm}^3$  as well as a low surface roughness of 10.56  $\mu\text{m}$  at 350 W laser power, 1000 mm/s scanning speed, 100  $\mu\text{m}$  hatching space, and 30  $\mu\text{m}$  layer height. The specimen 4 had an laser energy density of 63  $\text{J}/\text{mm}^3$ , a laser power of 250 W, a scanning speed of 1200 mm/s, a hatching distance of 110  $\mu\text{m}$ , a layer height of 30  $\mu\text{m}$ , and the maximum surface roughness at 11.34  $\mu\text{m}$ .

### 3.4 Signal to Noise Ratio

The impacting the input process variables were investigated and provided. A visual illustration of the impact of the regulating parameters on the specimens produced by SLM in terms of density, hardness, and surface roughness is presented in Fig. 3 (a). Investigations were conducted on the link between density and process factors such as laser power, scanning speed, hatch space, and layer height are all variables to consider, and it was

**Table 4:** Surface roughness Test Values

S.no	Power W	Laser Scan Speed mm/s	Hatch space $\mu\text{m}$	Layer height ( $\mu\text{m}$ )	Laser Energy Density in $\text{J}/\text{mm}^3$	Surface roughness, Ra ( $\mu\text{m}$ )
1	250	1000	90	30	93	10.98
2	300	1200	100	30	83	11.21
3	350	1400	110	30	76	11.26
4	250	1200	110	30	63	11.34
5	300	1400	90	30	79	11.03
6	350	1000	100	30	117	10.86
7	250	1400	100	30	60	11.24
8	300	1000	110	30	91	11.07
9	350	1200	90	30	108	10.88

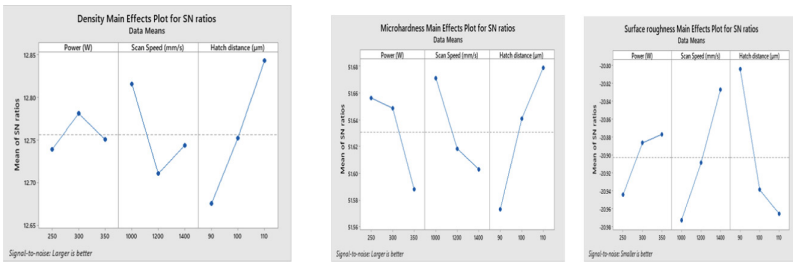


**Fig. 3** a) Density main effects plots b): Micro hardness Main effects plots c): Surface Roughness Main effects plots

found a higher density with an rise in power from 200 W to 300 W before decreasing at 350 W. Similarly, scan speed reveals its density first decreases from 1000 mm/s to 1200 mm/s before increase when it arrives at 1400 mm/s. The result of the hatch space reveals that it first grew from 90  $\mu\text{m}$  to 110  $\mu\text{m}$ . As illustrated in Fig. 3 (b), input process factors have an impact on hardness as well. Power increases from 250W to 350W reduce hardness, as does scan speed from 1000 mm/s to 1400 mm/s, whereas hatch distance increases from 90 $\mu\text{m}$  to 110  $\mu\text{m}$  enhance hardness. Figure 3 (c) illustrates the effects of the process parameters on Surface roughness varies from low to high between 250 and 350 W. At, the surface roughness is significant 1000 mm/s scan speed and low at 1200 mm/s scan speed. At a hatch distance of 90  $\mu\text{m}$ , surface roughness is modest, and at 110  $\mu\text{m}$ , it is high.

### 3.5 ANOVA Test

The correlation between production efficiency and process control variables could be determined using data study. The statistical method ANOVA was used to analyse the

**Table 5:** ANOVA on Density: Analysis of Variance on Density

Source	DF	Seq SS	Contribution	Adj SS	Adj MS	F-Value	P-Value
POWER	2	0.013889	73.79%	0.013889	0.006944	0.20	0.830
SCAN SPEED	2	0.000956	5.08%	0.000956	0.000478	1.28	0.439
HATCH DISTANCE	2	0.000156	0.83%	0.000156	0.000078	3.07	0.246
LAYER THICKNESS	2	0.003822	20.31%	0.003822	0.001911		
Error	0	*	*	*	*		
Total	8	0.018822	100.00%				

**Table 6:** Microhardness: Analysis of Variance on Microhardness

Source	DF	Seq SS	Contribution	Adj SS	Adj MS	F-Value	P-Value
POWER	2	256.676	89.23%	256.676	128.338	0.92	0.520
SCAN SPEED	2	19.056	6.62%	19.056	9.528	0.85	0.540
HATCH DISTANCE	2	11.376	3.95%	11.376	5.688	1.91	0.
LAYER THICKNESS	2	0.536	0.19%	0.536	0.268		
Error	0	*	*	*	*		
Total	8	287.642	100.00%				

acquired data, which analyzes the input process variables influence the range of responses as a whole. Statistical evaluation and response enhancement are done using the Minitab 19 application. On the measured data for density, surface roughness, and hardness, the ANOVA was performed. Following scan speed, power is the process parameter with the greatest influence, according to the ANOVA test for density. The microhardness is also influenced by the laser's intensity and scan speed. The main factors affecting surface roughness are input power and scan speed (Tables 5, 6, and 7).

## 4 Conclusions

Investigations were conducted on the impact of process variables by taking energy densities into account on the mechanical characteristics of Ti6Al4V ELI powders produced by selective laser melting. In this investigation, samples of the Ti6Al4V ELI alloy were created by changing the process parameters in nine Energy densities. To create high-quality products with this limitation, an appropriate ED range, or 49 to 97 J/mm<sup>3</sup>, was

**Table 7:** Surface Roughness: Analysis of Variance on Surface Roughness

Source	DF	Seq SS	Contribution	Adj SS	Adj MS	F-Value	P-Value
POWER	2	0.53502	72.11%	0.53502	0.26751	0.13	0.886
SCAN SPEED	2	0.11849	15.97%	0.11849	0.05924	0.52	0.659
HATCH DISTANCE	2	0.03616	4.87%	0.03616	0.01808	0.73	0.579
LAYER THICKNESS	2	0.05229	7.05%	0.05229	0.02614		
Error	0	*	*	*	*		
Total	8	0.74196	100.00%				

accomplished. A valuable SLM product was also created, and its relative density was high (99.54%). The main conclusions are summarized as follows:

1. The lowest recorded density was 4.301 g/cm<sup>3</sup>, While 4.410 g/cm<sup>3</sup> i.e. 99.54%, has the maximum density, was acquired at an energy density of 63 J/mm<sup>3</sup>. Power and layer thickness were the two process variables that were shown to be most important.
2. Input Laser power and scan speed had the greatest impact on Micro Hardness Properties The maximum hardness value is 386 HV, with an energy density of 63 J/mm<sup>3</sup>, and minimum hardness is 377 HV with a 108 J/mm<sup>3</sup> energy density.
3. Surface Roughness is stated to have a low value Ra of 10.86 μm with laser energy density of 79 J/mm<sup>3</sup>, and Ra of 11.34μm including an energy density of 63 J/mm<sup>3</sup>.
4. S/N Ratios demonstrate that power and layer thickness have the most effects on density, Power and scan speed have an effect on surface roughness. The input power has an effect on microhardness as well.
5. According to the variance test results, power and layer thickness have a significant impact on density, whereas input power and scan speed have the most impacts on surface roughness and micro hardness.

## References

1. Zhang, Wan-neng, et al. "Research Progress on Selective Laser Melting (SLM) of Magnesium Alloys: A Review." *Optik*, vol. 207, Apr. 2020, p. 163842. *ScienceDirect*, <https://doi.org/10.1016/j.ijleo.2019.163842>.
2. Singla, Anil Kumar, et al. "Selective Laser Melting of Ti6Al4V Alloy: Process Parameters, Defects and Post-Treatments." *Journal of Manufacturing Processes*, vol. 64, Apr. 2021, pp. 161–87. *ScienceDirect*, <https://doi.org/10.1016/j.jmapro.2021.01.009>.
3. Zhu Y, Zou J, yong Yang H. Wear performance of metal parts fabricated by selective laser melting: a literature review. *J Zhejiang Univ Sci A* 2018;19: 95–110. <https://doi.org/10.1631/jzus.A1700328>.
4. Yang L, Hsu K, Baughman B, Godfrey D, Medina F, Menon M, et al. Additive manufacturing of metals: the technology, materials, design and production. Springer; 2017.



5. Wang, Zhen, et al. "Optimization of Processing Parameters and Establishment of a Relationship between Microstructure and Mechanical Properties of SLM Titanium Alloy." *Optics & Laser Technology*, vol. 112, Apr. 2019, pp. 159–67. <https://doi.org/10.1016/j.optlastec.2018.11.014>.
6. Gupta MK, Singla AK, Ji H, Song Q, Liu Z, Cai W, et al. Impact of layer rotation on microstructure, grain size, surface integrity and mechanical behaviour of SLM Al-Si-10Mg alloy. *J Mater Res Technol* 2020; 9: 9506–22. <https://doi.org/10.1016/j.jmrt.2020.06.090>.
7. Shipley H, McDonnell D, Culleton M, Coull R, Lupoi R, O'Donnell G, et al. Optimisation of process parameters to address fundamental challenges during selective laser melting of Ti-6Al-4V: a review. *Int J Mach Tools Manuf* 2018; 128: 1–20. <https://doi.org/10.1016/j.ijmactools.2018.01.003>.
8. Zheng, Zhongpeng, et al. "Microstructure and Anisotropic Mechanical Properties of Selective Laser Melted Ti6Al4V Alloy under Different Scanning Strategies." *Materials Science and Engineering: A*, vol. 831, Jan. 2022, p. 142236. *ScienceDirect*, <https://doi.org/10.1016/j.msea.2021.142236>.
9. Song, Bo, et al. "Effects of Processing Parameters on Microstructure and Mechanical Property of Selective Laser Melted Ti6Al4V." *Materials & Design*, vol. 35, Mar. 2012, pp. 120–25. <https://doi.org/10.1016/j.matdes.2011.09.051>.
10. Praneeth, Jammula, et al. "Process Parameters Influence on Mechanical Properties of AlSi10Mg by SLM." *Materials Today: Proceedings*, Jan. 2023. *ScienceDirect*, <https://doi.org/10.1016/j.matpr.2022.12.222>.
11. Song, Bo, et al. "Effects of Processing Parameters on Microstructure and Mechanical Property of Selective Laser Melted Ti6Al4V." *Materials & Design*, vol. 35, Mar. 2012, pp. 120–25. <https://doi.org/10.1016/j.matdes.2011.09.051>.
12. Wang, Zhen, et al. "Optimization of Processing Parameters and Establishment of a Relationship between Microstructure and Mechanical Properties of SLM Titanium Alloy." *Optics & Laser Technology*, vol. 112, Apr. 2019, pp. 159–67. *DOI.org (Crossref)*, <https://doi.org/10.1016/j.optlastec.2018.11.014>.
13. Zheng, Zhongpeng, et al. "Microstructure and Anisotropic Mechanical Properties of Selective Laser Melted Ti6Al4V Alloy under Different Scanning Strategies." *Materials Science and Engineering: A*, vol. 831, Jan. 2022, p. 142236. *ScienceDirect*, <https://doi.org/10.1016/j.msea.2021.142236>.
14. He, Beibei, et al. "Microstructural Characteristic and Mechanical Property of Ti6Al4V Alloy Fabricated by Selective Laser Melting." *Vacuum*, vol. 150, Apr. 2018, pp. 79–83. *ScienceDirect*, <https://doi.org/10.1016/j.vacuum.2018.01.026>.

**Open Access** This chapter is licensed under the terms of the Creative Commons Attribution-NonCommercial 4.0 International License (<http://creativecommons.org/licenses/by-nc/4.0/>), which permits any noncommercial use, sharing, adaptation, distribution and reproduction in any medium or format, as long as you give appropriate credit to the original author(s) and the source, provide a link to the Creative Commons license and indicate if changes were made.

The images or other third party material in this chapter are included in the chapter's Creative Commons license, unless indicated otherwise in a credit line to the material. If material is not included in the chapter's Creative Commons license and your intended use is not permitted by statutory regulation or exceeds the permitted use, you will need to obtain permission directly from the copyright holder.

